Reduction of Structural Fe(III) in Nontronite by Humic Substances in the Absence and Presence of *Shewanella putrefaciens* and Accompanying Secondary Mineralization

Hongyan Zuo[a], Liuqin Huang[b] Rosalie K. Chu[c], Nikola Tolic[c], Nancy Washton[c], Zihua Zhu[c], Richard E. Edelmann[d], Samar Elagamy[e], Andre Sommer[e], Fubo Luan[f], Qiang Zeng[g], Yu Chen[g], Dafu Hu[g], Di Zhan[g], Jinglong Hu[g], and Hailiang Dong[a,g*]

[a]Department of Geology and Environmental Earth Science, Miami University, Oxford, OH 45056, USA

[b]State Key Laboratory of Biogeology and Environmental Geology, China University of Geosciences, Wuhan, 430074, China

[c]Environmental Molecular Sciences Laboratory, Pacific Northwest National Laboratory, Richland, Washington 99354, USA

[d]Center for Advanced Microscopy & Imaging, Miami University, Oxford, OH 45056, USA

[e]Molecular Microspectroscopy Laboratory, Department of Chemistry and Biochemistry, Miami University, Oxford, OH 45056, USA

[f]Research Center for Eco-Environmental Sciences
Chinese Academy of Sciences, Beijing, 100085, China

[g]State Key Laboratory of Biogeology and Environmental Geology, China University of Geosciences, Beijing 100083, China

Submitted to American Mineralogist

Dec 23, 2020

Table OM1 Magnitude-weighted parameters with errors representing the standard deviation for all formulas assigned (2.5 g/L HA concentration) for samples in bicarbonate buffer

	LHA GROUP				PPHA GROUP		
	NAu-2&LHA	NAu-2&LHA&heat-killed CN32	NAu-2&LHA&CN32		NAu-2&PPHA	NAu-2&PPHA&heat-killed CN32	NAu-2&PPHA&CN32
$(DBE)_w$	13.236	13.344	13.308		11.274	11.510	11.439
stdev	0.004	0.004	0.004		0.003	0.003	0.003
$(DBE/O)_w$	1.371	1.367	1.370		1.207	1.220	1.216
stdev	0.000	0.000	0.000		0.000	0.000	0.000
$(DBE-O)_w$	3.447	3.476	3.457		1.749	1.864	1.957
stdev	0.001	0.001	0.001		0.002	0.001	0.001
$(AI)_w$	0.307	0.316	0.316		0.122	0.131	0.144
stdev	0.000	0.000	0.000		0.000	0.000	0.000

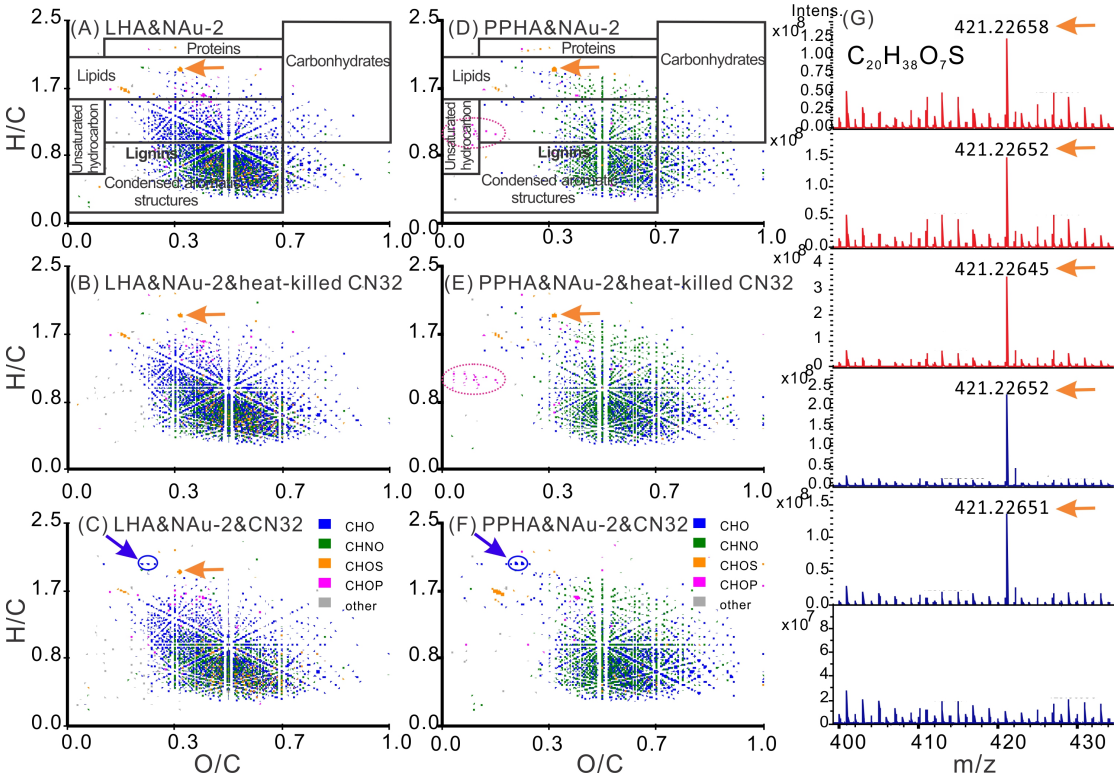

Figure OM1. van Krevelen diagrams for LHA (A-C) and PPHA (D-F) samples in bicarbonate buffer, along with several mass spectra (G) showing the *m/z* range of 400-430. (A) van Krevelen diagram of aqueous fraction of LHA after mixing with NAu-2, the diagram was divided into different regions, based on Hockaday et al. (2009) (B) Addition of heat-killed CN32 cells to LHA barely changed the composition of aqueous LHA. (C) With the addition of live CN32 cells, lipids $C_{11}H_{22}O_3$, $C_{12}H_{24}O_3$ and $C_{13}H_{26}O_3$ (indicated with blue arrow) emerged. (D) Aqueous fraction of PPHA after mixing with NAu-2. Compared with LHA (A), PPHA had CHOP compounds that are plotted in the area of unsaturated hydrocarbons (low O/C ratio, pink circle), fewer CHO compounds (blue), and more CHNO compounds (green). (E) Addition of heat-killed CN32 cells barely changed the composition of PPHA. (F) Live CN32 cells produced similar lipid products as in (C), but at the expense of unsaturated hydrocarbons (e.g., CHOP, the pink-circled compounds in D and E are no longer detected). (G) Mass spectra showing a $C_{20}H_{38}O_7S$ peak at *m/z* ~421.22, which corresponds to the compound labeled in (A)-(E) with a golden arrow. This compound disappeared after live cell treatment (F), suggesting a possibility of microbial consumption of this S-bearing compound in PPHA.

REFERENCES CITED

Hockaday, W.C., Purcell, J.M., Marshall, A.G., Baldock, J.A., and Hatcher, P.G. (2009) Electrospray and photoionization mass spectrometry for the characterization of organic matter in natural waters: a qualitative assessment. Limnology and Oceanography: Methods, 7(1), 81-95.